

Stellar radii from long-baseline interferometry

Pierre Kervella

LESIA, Observatoire de Paris, CNRS UMR 8109, UPMC, Université Paris Diderot,
5 Place Jules Janssen, 92195 Meudon, France
email: Pierre.Kervella@obspm.fr

Abstract. Long baseline interferometers now measure the angular diameters of nearby stars with sub-percent accuracy. They can be translated in photospheric radii when the parallax is known, thus creating a novel and powerful constraint for stellar models. I present applications of interferometric radius measurements to the modeling of main sequence stars. Over the last few years, we obtained accurate measurements of the linear radius of many of the nearest stars: Procyon A, 61 Cyg A & B, α Cen A & B, Sirius A, Proxima... Firstly, I describe the example of our modeling of Procyon A (F5IV-V) with the CESAM code, constrained using spectrophotometry, the linear radius, and asteroseismic frequencies. I also present our recent results on the low-mass 61 Cyg system (K5V+K7V), for which asteroseismic frequencies have not been detected yet.

Keywords. techniques: interferometric, stars: individual (Procyon, 61 Cyg), stars: evolution

1. Introduction

Long-baseline interferometry now routinely provides stellar angular diameters with sub-percent accuracy. These measurements are independent from the classical observables obtained by photometry or spectroscopy, and therefore represent a very valuable addition to constrain the stellar evolution and structure models. After a short description of the principle of interferometric angular size measurements (Sect. 2), I present in Sect. 3 the results we obtained on the benchmark star Procyon A. This star is specially interesting as a number of seismic oscillation frequencies have been detected by spectroscopy, and I discuss the synergy between the interferometric radius measurement and asteroseismology. Section 4 is then dedicated to the discussion of our most recent results on the low-mass binary star 61 Cyg.

2. Visibilities and angular diameters: a brief interferometry primer

This article is not intended to give an extensive tutorial on optical long-baseline interferometry, but rather explain its general principle with simplified concepts. For the interested reader, several excellent introductions to interferometry are available either in publications (Lawson *et al.* 2000; Perrin & Malbet 2003; Malbet & Perrin 2007) or through specialized web sites (OLBIN 2008; JMMC 2008).

An interferometer can be defined as a non-connex pupil telescope, i.e. a telescope whose pupil is split in a number of separate pieces. This simple definition can be used to better understand the angular resolution of an interferometer from its point spread function (PSF). Let's first consider the PSF of a single-dish telescope equipped with a primary mirror of diameter $D = 10$ m, no central obscuration and no atmospheric perturbation (or with a perfect adaptive optics system). The Rayleigh resolution criterion states that such a telescope is able to separate details that are $\theta_{\text{tel}} = 1.22 \lambda/D = 55$ milliarcseconds

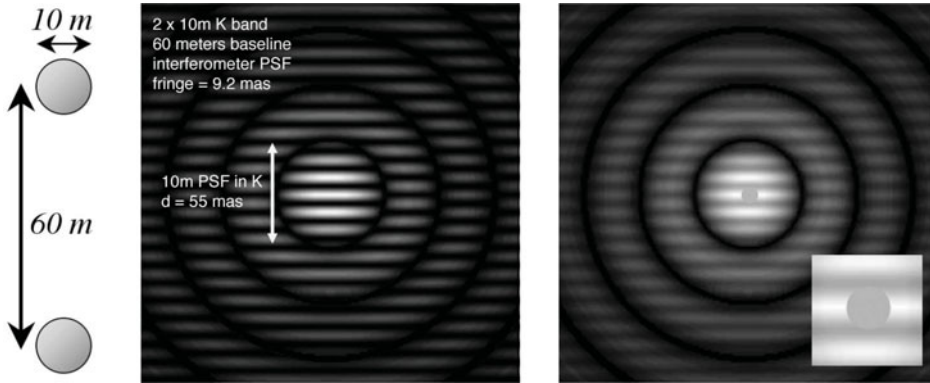


Figure 1. *Left:* Pupil of an interferometer of two 10 m telescopes separated by 60 m. *Middle:* Point Spread Function of this interferometer, when operated in the *K* band. The fringe spacing is 9.2 mas. *Right:* Image of α Cen A ($\theta \approx 8.5$ mas) formed by this interferometer, with the superimposed stellar disk. The fringes have a lower contrast than on the left, as the star is partially resolved. As shown in the insert on the right, the light from the stellar disk “leaks” in the dark fringes.

(mas) apart on the sky, in the *K* band ($\lambda = 2.2 \mu\text{m}$). As a comparison, the largest solar-type star angularly is α Cen A, with $\theta \approx 8.5$ mas, i.e. more than six times smaller than the resolution limit of the telescope. Now let’s consider the PSF of an interferometer of two 10 m telescopes separated by a baseline of 60 m (Fig. 1, left). As this setup is a particular case of the classical Young’s experiment, the diffraction pattern of this instrument is made of a series of interference fringes superimposed on the PSF of an individual telescope. Thanks to the long baseline, the spacing of the interference fringes is 6 times smaller than the single telescope PSF along the direction of the baseline (Fig. 1, middle), and corresponds to a resolution of 9.2 mas. Although this value is still a bit larger than α Cen A, it becomes comparable, and the image formed by the interferometer (Fig. 1, right) is now significantly different from the PSF. The finite angular size of α Cen A causes a reduction of the contrast of the fringes, that can be measured with great accuracy. There is a direct relation between the visibility of the fringes and the angular size of the star (Zernike-Van Cittert theorem), that allows to retrieve the angular size of the star. The best interferometric instruments currently available can provide contrast measurements with a relative precision of $\approx 0.1\%$, and angular diameters to $\pm 0.1\%$ or better. Intuitively, the reason for the change of the contrast with the increasing resolution is that the size of the star becomes larger than the spacing of a fringe, and its flux starts to “leak” in the dark fringes flanking the bright central fringe.

Naturally, interferometry does not provide direct *radius* measurements. In order to retrieve the linear photospheric size of a star, one needs its parallax. Thanks to the *Hipparcos* catalogue (ESA 1997), most nearby stars have high accuracy parallaxes. However, one should keep in mind that their accuracy can still be limiting to compute the radius, particularly when the angular diameter is known with very high accuracy ($\lesssim 1\%$).

3. Procyon A: the synergy of interferometry and asteroseismology

Procyon A is among the brightest stars in the sky and is easily visible to the naked eye. This made it an ideal target for a number of spectro-photometric calibration works. It is also a visual binary star classified F5IV-V, with a white dwarf (WD) companion orbiting the main component in 40 years. The influence of this massive companion on the

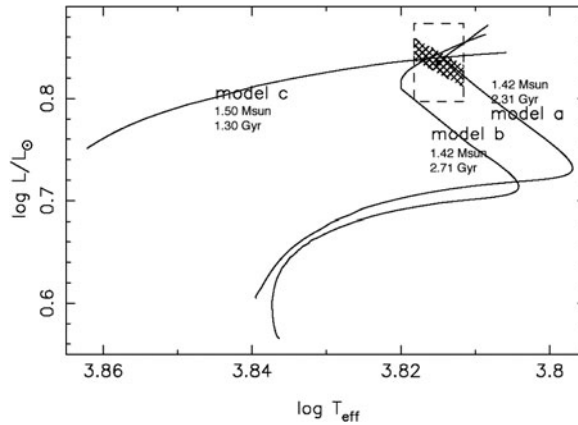


Figure 2. *Left:* Evolutionary tracks of three models of Procyon in the Hertzsprung-Russell diagram. *Right:* Corresponding model parameters (Kervella *et al.* (2004)).

apparent motion of Procyon was discovered by Bessel (1844), and Girard *et al.* (2000) obtained astrometric masses of $1.497 \pm 0.037 M_{\odot}$ and $0.602 \pm 0.015 M_{\odot}$, respectively for Procyon A and B. It has also been an asteroseismic target for a decade and Martić *et al.* (1999; 2001) measured a large frequency spacing of 54–55 μHz .

In Kervella *et al.* (2004), we presented several models of Procyon computed with the CESAM code (Morel 1997; Morel & Lebreton 2007). Because numerous new studies and observational constraints (like the direct diameter) exist today, we re-examined the status of Procyon. Our models were constrained using the spectroscopic effective temperature and the linear diameter value that we derived from our observations with the VINCI/VLTI instrument (Kervella *et al.* 2000; 2003a). Figure 2 (left) shows the evolutionary tracks of three models that converge into the uncertainty box in the HR diagram. The corresponding parameters are listed in the table of Fig. 2 (right). The added value of interferometry is clearly visible on this diagram, as the surface of the diagonal shaded area, set by the constraint from the interferometric radius, is much smaller than the classical $L - T_{\text{eff}}$ uncertainty box represented as a rectangle. More generally, the radius constraint always appears as a diagonal zone in the classical $L - T_{\text{eff}}$ HR diagram with logarithmic scales, as the photospheric radius is linked to these two quantities by Stefan-Boltzmann's law: $L = 4\pi R^2 \sigma T_{\text{eff}}^4$. From this law, a $10\times$ increase in the radius of a star causes a $100\times$ increase in luminosity (at constant T_{eff}) or a $\sqrt{10}\times$ decrease in T_{eff} (at constant L).

Although our model *c* converges in the radius-limited uncertainty domain of the HR diagram (Fig. 2, left), the associated large frequency spacing of 56.4 μHz is too large compared to the values measured by Martić *et al.* ($\Delta\nu_0 \sim 54 - 55 \mu\text{Hz}$). Moreover, the corresponding model age of 1.3 Gyr is too young for the cooling time of the white dwarf Procyon B. Provencal *et al.* (2002) found that its progenitor ended its lifetime 1.7 ± 0.1 Gyr ago, an age incompatible with the 1.3 Gyr of model *c* and thus with the $1.50 M_{\odot}$ mass of Procyon A from Girard *et al.* (2000). By reducing the mass of Procyon to $1.42 M_{\odot}$ (models *a* and *b*), we could reproduce both the observed radius and seismic large frequency spacing accurately. For our preferred model *a* of Procyon A, we derive an age of 2 314 Myr. Subtracting the cooling age of the WD companion to our determination of the age of Procyon A leads to a lifetime of ≈ 600 Myr for the progenitor of Procyon B. This indicates that the mass of the progenitor is approximately $2.5 M_{\odot}$. Such a star is expected to evolve towards a $\approx 0.6 M_{\odot}$ white dwarf, just as Procyon B, thus strengthening

our coherent picture of this stellar system. Two years after the publication of our work in 2004, Gatewood & Han (2006) redetermined the astrometric mass of Procyon, and found $M = 1.43 \pm 0.03 M_{\odot}$, in excellent agreement with our “interfero-seismic” modeling.

An extensive review of the remarkable synergy between interferometry and asteroseismology is given by Cunha *et al.* (2007). Kjeldsen & Bedding (2003) showed that the large frequency spacing $\overline{\Delta\nu_0}$ is proportional to the square root of the density of the star: $\overline{\Delta\nu_0} \sim 134.9 \sqrt{(m/M_{\odot})/(R_*/R_{\odot})^3}$ [μHz]. From this expression, it is clear that the interferometric radius, combined with $\overline{\Delta\nu_0}$ brings a strong constraint on the mass of the star. But interferometry is not only useful for measuring stellar radii: it can also efficiently constrain the stellar atmosphere structure from limb darkening measurements. The interested reader can refer to Aufdenberg *et al.* (2005) for a comparison of the limb darkening predictions of several models of the atmosphere of Procyon with interferometric visibility measurements obtained over a broad range of wavelengths.

4. 61 Cyg A & B: a low-mass nearby binary system

The cool dwarfs 61 Cyg A and B are the nearest stars in the northern hemisphere. They are a visual binary pair with a very long orbital period (≈ 700 yrs). In 1838, 61 Cyg became the first star whose distance from Earth was estimated accurately (Bessel 1838), shortly before Procyon’s, and it is now known with an exquisite accuracy. Its proper motion of more than $5''$ per year, first determined by Piazzini in the XVIIIth century, makes it one of the fastest moving stars in terms of apparent displacement. Although some of this motion comes from the proximity of 61 Cyg to us, the pair is also moving fast into space relative to the Sun, at 108 km/s, indicating that 61 Cyg is not a member of the thin disk of our Galaxy. The proximity of 61 Cyg makes it a northern analog of the numerical modeling benchmark α Cen. The spectral types of its two members (K5V and K7V) ideally complement our previous studies of α Cen A & B (G2V+K1V; Kervella *et al.* 2003b; Bigot *et al.* 2006). The masses of 61 Cyg A & B are controversial at approximately 0.74 and 0.46 M_{\odot} (Gorshanov *et al.* 2006) or 0.67 and 0.59 M_{\odot} (Walker *et al.* 1995). With effective temperatures of about 4400 and 4000 K, they shine at luminosities of only 0.15 and 0.08 L_{\odot} . There is no confirmed planet around them, although indications exist that 61 Cyg B could host a giant planetary companion (Gorshanov *et al.* 2006). The abundances of heavy chemical elements have been determined (Luck & Heiter 2005, 2006) in these stars which are found slightly metal poor (≈ -0.2 dex), so a priori older than the Sun but belonging to the galactic disk.

The measured CHARA/FLUOR visibilities translate into the following angular diameters: $\theta_{\text{LD}}(61 \text{ Cyg A}) = 1.775 \pm 0.013$ mas, $\theta_{\text{LD}}(61 \text{ Cyg B}) = 1.581 \pm 0.022$ mas. The limb darkening (LD) models were taken from Claret (2000) for the K band. From the combination of these angular diameters and the trigonometric parallaxes taken from van Altena *et al.* (1995) for 61 Cyg A and the *Hipparcos* catalogue (ESA 1997) for 61 Cyg B ($\pi_A = 286.9 \pm 1.1$ mas, $\pi_B = 285.4 \pm 0.7$ mas), we derive the following photospheric linear radii: $R(61 \text{ Cyg A}) = 0.665 \pm 0.005 R_{\odot}$, $R(61 \text{ Cyg B}) = 0.595 \pm 0.008 R_{\odot}$. The relative uncertainties on the radii are therefore $\pm 0.8\%$ and $\pm 1.4\%$. Thanks to the high precision of the parallaxes (0.38% and 0.25%), the radius accuracy is limited in this case by the precision of the angular diameter measurements.

Using the available classical constraints (photometry, spectroscopy) and the radii, we computed a series of CESAM2k models (Morel & Lebreton 2007). We selected as the most plausible models those satisfying first the luminosity and radius constraints and second the effective temperature constraint. The models of 61 Cyg A and B converge simultaneously to the radii-limited uncertainty boxes for masses of 0.69 and 0.61 M_{\odot}

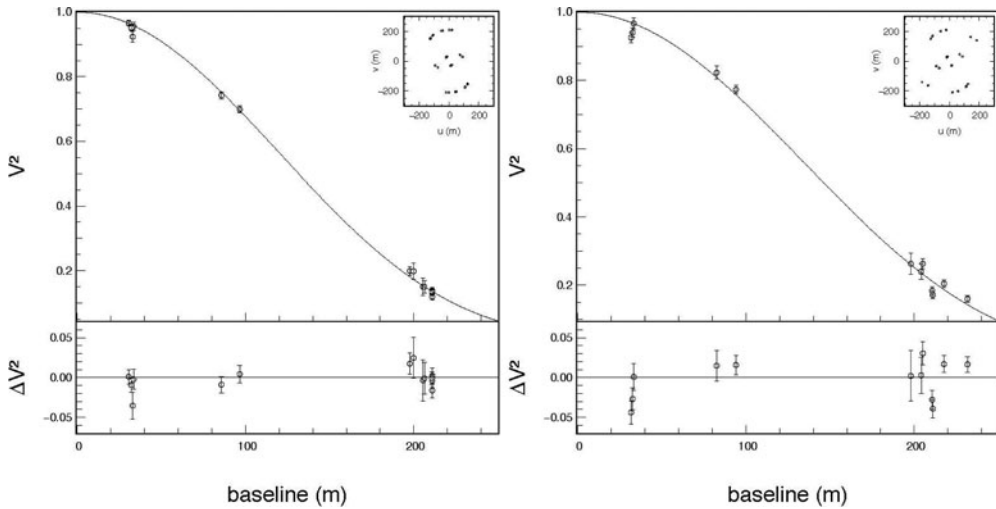


Figure 3. Visibility data from CHARA/FLUOR interferometric measurements (open circles) and the adjusted limb darkened disk model visibility curves (solid curves) for 61 Cyg A (left) and B (right) from Kervella *et al.* (2008).

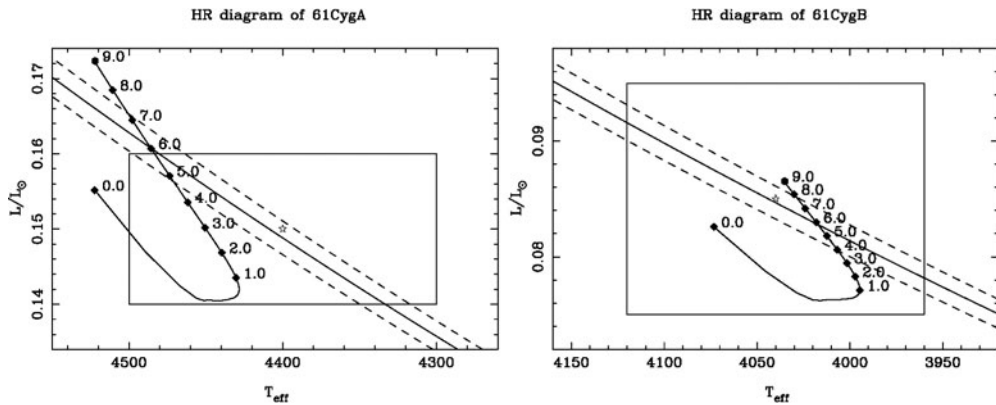


Figure 4. CESAM2k evolutionary tracks of 61 Cyg A (left) and B (right). The labels indicate the age in Gyr relatively to the ZAMS. The rectangular box represents the classical $L - T_{\text{eff}}$ error box, and the diagonal lines represent the radius and its uncertainty.

and an age of 6.0 ± 1.0 Gyr (Fig. 4). However, it appears difficult to go beyond the present modeling of the binary system. The main reason is that the masses are presently not constrained sufficiently well by the long period astrometric orbit, and no seismic frequencies have been detected yet in this system. The detection of such oscillations would bring precious constraints to stellar structure models in the cool, low-mass part of the HR diagram.

5. Conclusion

We presented two examples of stellar evolution modeling constrained by interferometric radius measurements: Procyon A and 61 Cyg A & B. In both cases, the radius reduces spectacularly the error boxes in the HR diagram, and thus brings a strong constraint on the evolutionary status of the stars. But, as shown by our Procyon modeling and Cunha *et al.* (2007), the best results are obtained when asteroseismic frequencies are available.

In this case, the radius and frequencies combine to constrain the mass of the system very tightly (Creevey *et al.* 2007). Several hundred stars are accessible to high accuracy radius measurements to 3% or better by interferometry, and even more will soon be within reach of the new generation of interferometric facilities. So one can expect new and exciting results in this field in a near future.

Acknowledgements

This research took advantage of the SIMBAD and VIZIER databases at the CDS, Strasbourg (France), and NASA's Astrophysics Data System Bibliographic Services.

References

- Aufdenberg, J. P., Ludwig, H.-G., & Kervella, P. 2005, *ApJ*, 633, 424
 Bessel, F. W. 1838, *MNRAS*, 4, 152
 Bessel, F. W. 1844, *MNRAS*, 6, 136
 Bigot, L., Kervella, P., Thévenin, F., & Ségransan, D. 2006, *A&A*, 446, 635
 Claret, A., 2000, *A&A*, 363, 1081
 Creevey, O. L., Monteiro, M. J. P. F. G., Metcalfe, T. S., *et al.* 2007, *ApJ*, 659, 616
 Cunha M. S., Aerts C., Christensen-Dalsgaard J., Baglin A., *et al.* 2007, *A&ARv*, 14, 217
 ESA 1997, The Hipparcos and Tycho Catalogues, ESA SP-1200
 Gatewood, G. & Han, I. 2006, *AJ*, 131, 1015
 Girard, T. M., Wu, H., Lee, J. T., *et al.* 2000, *AJ*, 119, 2428
 Gorshanov, D. L., Shakht, N. A., & Kisselev, A. A. 2006, *Ap*, 49, 386
 JMMC, Jean-Marie Mariotti Center web site, <http://www.mariotti.fr/>
 Kervella, P., Coudé du Foresto, V., Glindemann, A. & Hofmann, R. 2000, *SPIE*, 4006, 31
 Kervella, P., Gitton, Ph., Ségransan, D., *et al.* 2003a, *SPIE*, 4838, 858
 Kervella, P., Thévenin, F., & Ségransan, D., *et al.* 2003b, *A&A*, 404, 1087
 Kervella, P., Thévenin F., Morel, P., *et al.* 2004, *A&A*, 413, 251
 Kervella, P., Mérand, A., Pichon, B., *et al.* 2008, *A&A*, submitted
 Kjeldsen, H., & Bedding, T. 1995, *A&A*, 293, 87
 Lawson, P. (ed.) 2000, Course Notes from the 1999 Michelson Summer School, JPL Pub. 00-09
 Luck, R. E., & Heiter, U. 2005, *AJ*, 129, 1063
 Luck, R. E., & Heiter, U. 2006, *AJ*, 131, 3069
 Malbet, F., & Perrin, G. (eds.) 2007, *New Astronomy Reviews*, 51, 8-9, 563, Proceedings of the EuroSummer School "Observation and Data Reduction with with the VLT Interferometer" (<http://ultischool.obs.ujf-grenoble.fr>)
 Martic, M., Schmitt, J., Lebrun, J., *et al.* 1999, *A&A*, 351, 993
 Martic, M., Lebrun, J.-C., Schmit, J., Appourchaux, Th., & Bertaux, J.-L. 2001, in SOHO 10 / GONG 2000 Workshop, A. Wilson ed., ESA SP-464, p 431
 Morel, P. 1997, *A&AS*, 124, 597
 Morel, P., & Lebreton, Y. 2007, *Ap&SS*, doi:10.1007/s10509-007-9663-9
 OLBIN, Optical Long Baseline Interferometry News web site, <http://olbin.jpl.nasa.gov/>
 Perrin, G., & Malbet, F. (eds.) 2003, *EAS Publications Series*, 6, Proceedings of the EuroWinter School "Observing with the VLTI", <http://www.mariotti.fr/obsvlti/obsvlti-book.html>
 Provencal, J. L., Shipman, H. L., Koester D., Wesemael, F. & Bergeron, P. 2002, *ApJ*, 568, 324
 Van Altena, W. F., Lee, J. T., & Hoffleit, E. D. 1995, *The General Catalogue of Trigonometric Stellar Parallaxes*, Fourth Edition, Yale University Observatory
 Walker, G. A. H., Walker, A. R., Irwin, A. W. *et al.* 1995, *Icarus*, 116, 359

Discussion

WOITKE: Your analysis works best for "clean stars". One should be aware that K-band interferometry is quite sensitive to e.g. close circumstellar material, hot dust, etc., which can lead to misleading conclusions, in particular for red giants.

KERVELLA: (1) Dust, e.g., in disks, emits at longer wavelengths and is usually not a problem in the K-band. (2) This is a very good point, however, specifically for dusty envelopes around evolved stars, that can have a significant impact on the radius estimation.

STEPIEN: Is it true that all existing models of low mass main sequence stars show systematically smaller radii than observed?

KERVELLA: I am not an expert in this field of stellar modeling, but it is clear that the adjustment of some parameters related in particular to the treatment of convection would possibly improve the agreement with the models. Such models certainly are possible, but I am not aware of them.

LUDWIG: In view of the systematic differences of the stellar radii at low T_{eff} between the measurements and theoretical mass-radius relationship: Have the stellar structure models been calculated assuming a constant-presumably solar calibrated-mixing length parameter? Remark on interferometric measurements: For constraining stellar atmosphere models visibilities at optical (or even shorter!) wavelength are particularly valuable.

KERVELLA: (1) Yes, as far as I can tell, the models were computed assuming a constant value of the MLT parameter. (2) Indeed! Measurements of the limb darkening at visible wavelength would be very useful. But due to turbulence, that is stronger in the visible, these measurements are significantly more difficult to obtain there in the infrared.

FERNANDES: I wonder if the claimed disagreement between models and observations in the mass-radius diagram (at the low mass regime) is mainly related with activity more than convection.

KERVELLA: This is a very good point. The low mass dwarfs with spectral types K and M tend to show rather strong magnetic activity (flares in particular), that can possibly bias the T_{eff} and L estimates. However, interferometric measurements are relatively insensitive to these perturbations.